

---

---

# Geology of the Chukar Footwall Mine, Maggie Creek District, Carlin Trend, Nevada: A progress report

Juan Ruiz Parraga\*

*The Ralph J. Roberts Center for Research in Economic Geology, University of Nevada-Reno, Reno, Nevada 89557*

---

## ABSTRACT

The Chukar Footwall mine forms part of the NW striking Carlin trend in northern Nevada, and lies beneath the southwest highwall of the Gold Quarry, a world-class deposit with total 1999 reserves, resources, and mineral inventories in excess of 24M oz gold. The Chukar Footwall orebodies are hosted in the planar to wispy silty limestone and calc-silicates of the Silurian-Devonian Roberts Mountains Formation (SDrm). The Devonian Popovich Formation (Dp), a micritic package locally hosting economic gold mineralization, structurally overlies the DSrm. The Raven dike intrudes the DSrm at several mine levels along northwest-trending structures. The dike is composed of abundant dark green, millimeter sized subhedral-anhedral phenocrysts in a light colored aphanitic groundmass. It is altered to clay and pyrite, but does not appear to be a feeder structure. These rocks were deformed during the Antler orogeny, generating the Chukar anticline, a northeast trending open structure with a subhorizontal plunge. High gold grades are commonly situated along the hinge and the southeast limb and in small parasitic folds. A conjugate system of structures is represented by northwest and northeast striking faults, where the former cuts the latter. Kinematic indicators denote predominantly oblique normal slips for both fault sets.

Geochemical analyses show that As, Fe, and Sb have a high correlation with Au, whereas Ag and Ba have a weak correlation with this element. Finally, pyrite and stibnite are the most common sulfides. Arsenic minerals are scarce, occurring in the deeper mine levels replacing decalcified rock. Calcite occurs as multistage veins, stockworks, and in vugs.

The Chukar Footwall mine exhibits the hydrothermal alteration assemblages typical of Carlin-type gold deposits: (a) decalcification, (b) dolomitization, (c) silicification, and (d) baritization. The uniqueness of this deposit relative to the more typical Carlin-type is the (1) sharp boundaries between fresh and altered rocks, and (2) presence of abundant visible gold. Gold mineralization is spatially related with strong decalcification in the vicinity of intersections of northeasterly structures with the Chukar anticline. Coarse gold occurs in decarbonatized silty limestone along fractures of all orientations as well as along bedding planes. Also, visible gold is present in late barite veinlets, coprecipitating with the latter phase.

**Key Words:** Chukar Footwall mine, Carlin Trend, Chukar anticline, Roberts Mountains Formation, structural framework, decarbonatization, silicification, visible gold.

---

\*E-mail, parraga@unr.edu

## INTRODUCTION

The discovery in 1995 of the Chukar Footwall orebody beneath the southwest highwall of the Gold Quarry mine brought out the potential to explore for deep blind deposits along the Carlin trend in northeastern Nevada (Fig. 1). The Carlin trend is a north-northwest trending belt with a mineral endowment of more than 50 million ounces gold produced between 1965 and 2002 (Teal and Jackson, 2002). After a period of near-surface exploration, current exploration projects are focused on deeper, blind orebodies through both direct and indirect methods. No geological data about the blind orebodies can be inferred from surface outcrops, thus the structure and geochemistry of the orebody is deduced from drill data (i.e., West Leeville, Chukar Footwall).

The detailed stratigraphy, structure, and metallogeny of the Carlin trend are well known at both regional scale and deposit scale. The tectonic evolution of this area indicates a complex scenario through time involving widespread Early Silurian to Late Devonian-Mississippian shallow to deep water carbonate depositional environments deposited on to the Cordilleran passive margin; traditionally this package of rocks have been referenced as the miogeoclinal strata. Coeval eugeoclinal strata were deposited further west from the margin, and thrust over the miogeoclinal sequences during the Late Devonian-Early Mississippian Antler orogeny along the Roberts Mountains thrust (Roberts and others, 1958; Cook and Corboy, 2004). During pre-Tertiary times, this region underwent several compressional phases giving rise to large WNW to NNW trending folds (i.e., Post anticline, Tuscarora anticline, and Betze anticline) with associated minor structures (Lewis, 2001). Dioritic, quartz-dioritic, and granodioritic bodies and associated sills and dike swarms were emplaced at 158 Ma and 106 Ma (Evans, 1980; Emsbo and others, 1996) producing significant contact metamorphism and metasomatism in the host lithologies. Tectonic history is mainly represented by the (1) reactivation of older structures, (2) emplacement of Eocene dikes, which are interpreted to be contemporaneous with gold mineralization in some districts (Henry and Ressel, 2000; Heitt and others, 2003; Mariño, 2003), and (3) Miocene Basin and Range extension (Arehart, 1996; Emsbo and others, 1996).

The Carlin trend displays several general metallogenic characteristics (Roberts, 1960; Hofstra and Cline, 2000; Thompson, 2000): (1) the host rocks are lower plate Paleozoic carbonates, which are exposed along an north-northwest alignment through several tectonic windows; however, some orebodies occur in different lithologies; (2) temporally and spatially linked with gold orebodies, the hydrothermal alteration assemblages are represented by decarbonatization  $\pm$  dolomitization  $\pm$  silicification  $\pm$  argillization  $\pm$  sulfidation and baritization  $\pm$  alunization and supergene processes; and (3) gold occurs as sub-microscopic grains disseminated along arsenian rims on iron sulfide minerals. Common ore and gangue mineralogies are represented by barite, calcite, quartz, stibnite, iron sulfides, fluorite, realgar, and orpiment.

There are currently several competing models attempting to explain the genesis of the Carlin-type gold deposits. Central to this controversy is the question of the metal source and heat mechanisms: (1) fluids and metals were derived during regional metamorphism of crustal rocks during an Eocene extensional event (Seedorff, 1991), (2) meteoric fluids were heated and convected during rapid crustal extension during Basin and Range extension (Ilchick and Barton, 1997), (3) due to the spatial association of some Carlin-type deposits with igneous rocks some authors suggest a magmatic provenance of fluids and metals (Arehart and others, 1993, Radke, 1985, Thompson, 2000), and (4) recently, Johnston and Ressel (2004) suggested the possibility that Carlin-type deposits may be interpreted as distal and shallow expression of a deeper magmatic system(s) underlying the trend due to their temporal coincidence with regional Eocene magmatism.

In this paper, with the specific purpose of a progress report, the geologic framework of the Chukar Footwall mine is described based on underground mapping, geochemical and structural data. These data provide additional information on the geologic realm of the Carlin-type deposits in north-central Nevada and allow us to make some comparisons.

## GEOLOGY OF THE CHUKAR FOOTWALL MINE

### Lithostratigraphic Setting of the Chukar Footwall Deposit

The Chukar Footwall orebody lies beneath the southwest highwall of the Gold Quarry mine in the footwall of the Chukar Gulch fault (Fig. 2), a NE striking fault dipping 65° SE that may be interpreted as a structural domain boundary for the deposit (Sagar, 2000b). The Gold Quarry deposit have mainly been described by Rota and Hausen (1991), Williams (1992), Sha (1993), Cole (1995), and Harlan and others (2002). The stratigraphic sequence at Chukar Footwall is comprised of silty carbonates of the miogeoclinal facies wherein the economic orebodies, outlined by a 0.20 opt Au cutoff, are hosted in the Silurian-Devonian Roberts Mountains Formation.

Contact metamorphism gave rise to grey-green pyroxene hornfels, overprinting original carbonate textures and, locally, generating coarse mottle-textured vesuvianite grains along former bedding planes. The blind plutonic intrusion responsible for this thermal phenomenon is unknown. Drill hole data (Fig. 11) suggest an intrusive body toward the WNW, because the metamorphic thermal effects increase with the appearance of new mineral phases and Zn sulfide. This setting is similar to the one observed in rocks of the nearby Mike (Soap Creek) deposit described by Norby and Orobona (2002), wherein the Cretaceous Richmond stock was responsible for the thermal event and associated base metal-Bi-W-Mo mineralizations. Likewise, the thermal event observed at Chukar Footwall deposit may also be the result of the Eocene metamorphism correlative with the intrusion of the Welches Canyon stock to the west of Gold Quarry.

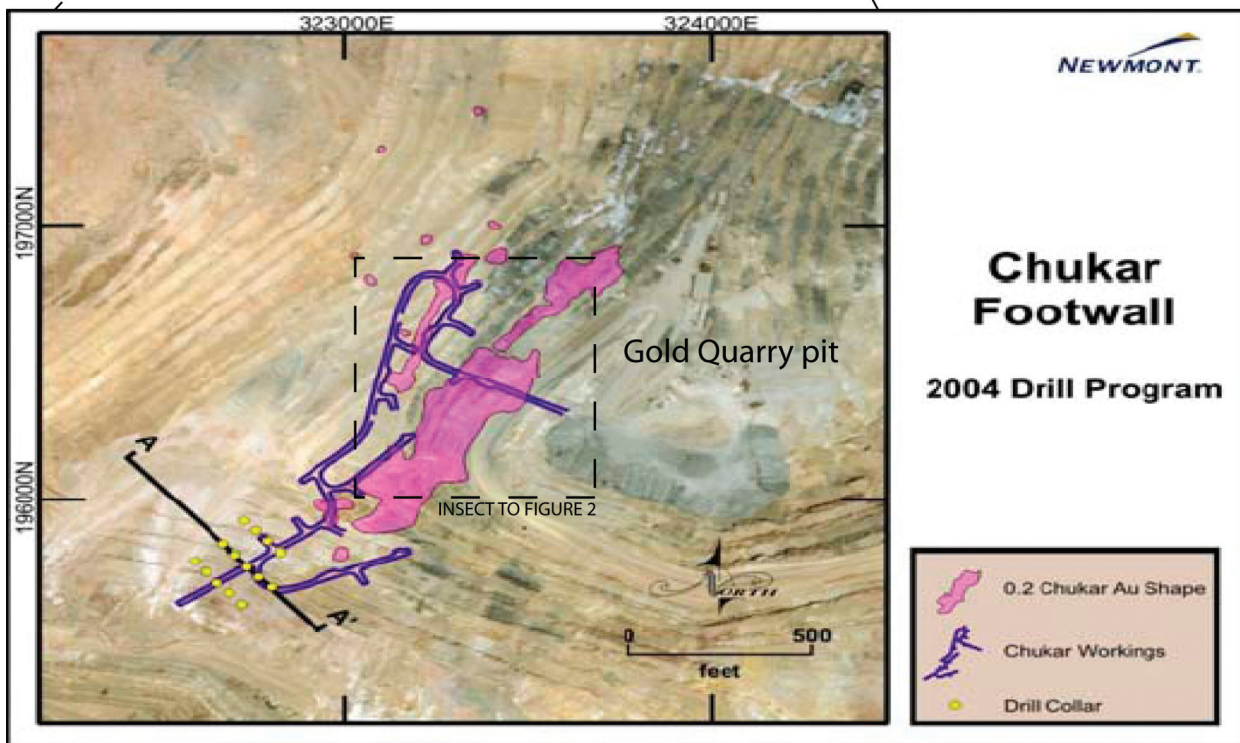
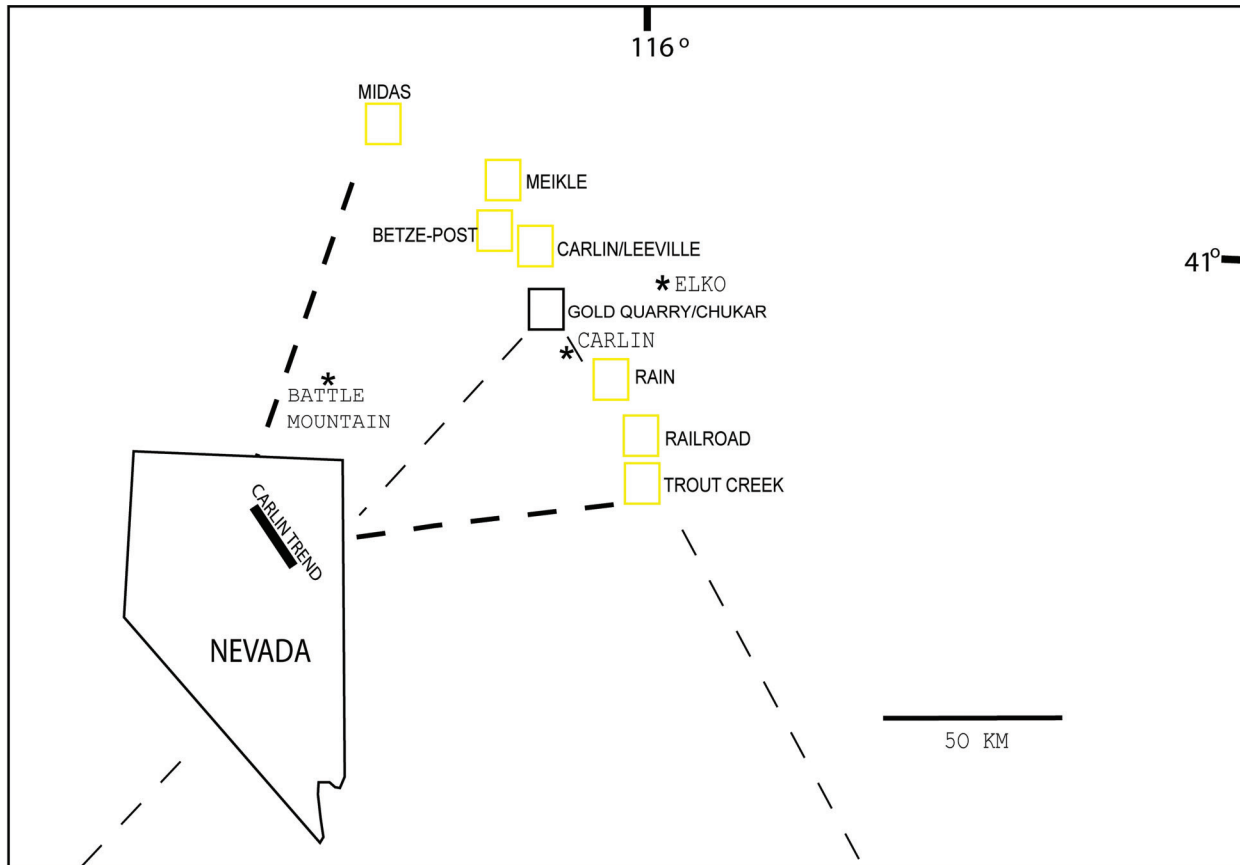


Figure 1. Location map of the Carlin trend in northeastern Nevada, a NNW-trending series of gold deposits hosted in Paleozoic carbonate rocks and mined by open pits and underground methods. The Chukar Footwall underground mine is located beneath the southwest highwall of the Gold Quarry pit.

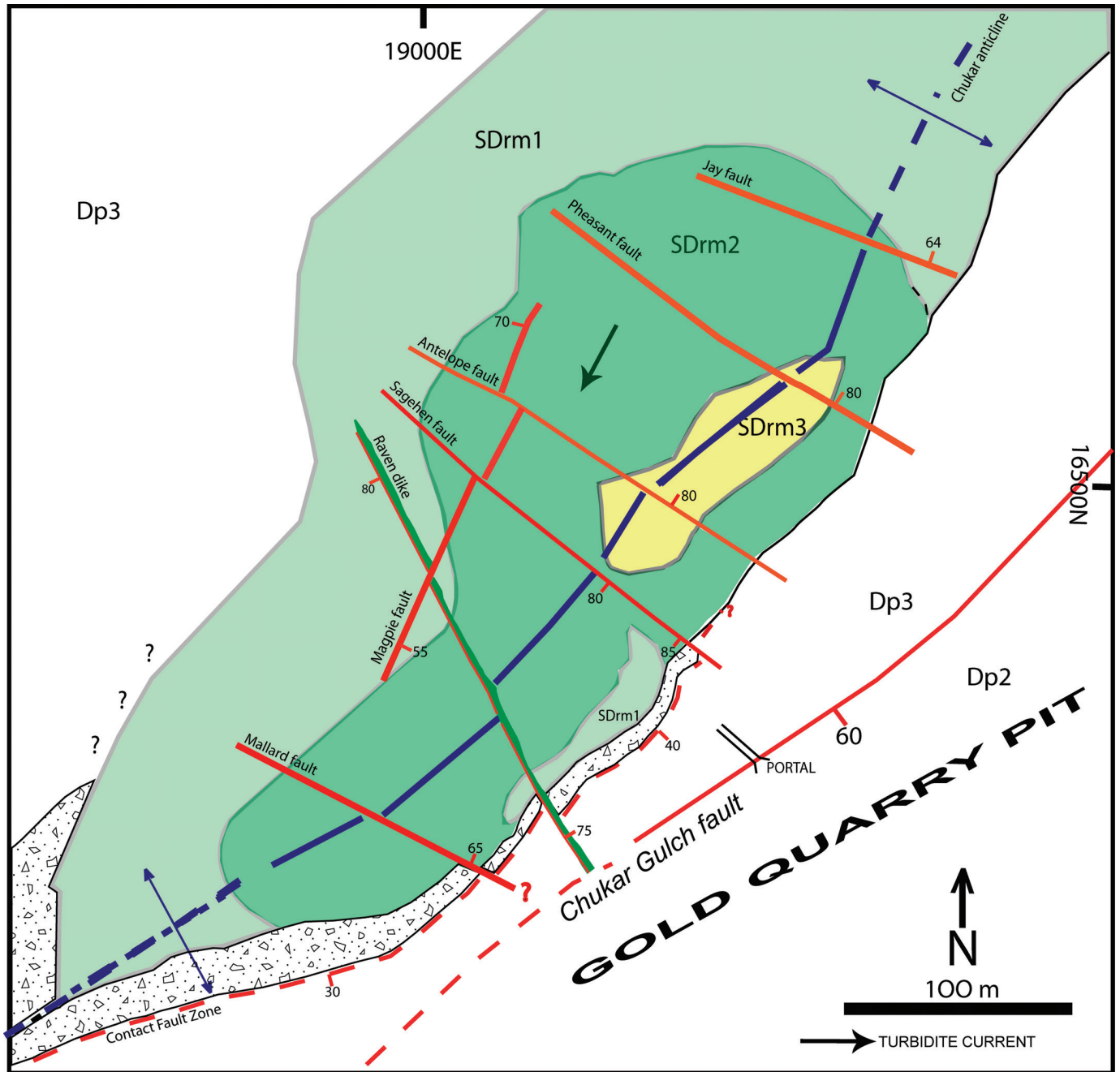


Figure 2. Simplified geologic map of the Chukar Footwall mine at the 4650 level. The Devonian-Silurian Roberts Mountains Formation (SDrm) is the main host rock for disseminated gold mineralizations. The geometry of the Contact Fault Zone, interpreted as a low angle normal fault, is still poorly constrained along the crest and west limb of the Chukar anticline. The Devonian Popovich Formation (Dp2,Dp3) is a monotonous package of massive, dark to grey micrites ( Modified from Newmont, 2003).

### **Silurian-Devonian Roberts Mountains Formation**

The Roberts Mountains Formation (DSrm) consists of thin to relatively thick-bedded to laminated silty limestone of middle Silurian-early Devonian age (Evans, 1980; Mullens, 1980). Regionally, the DSrm has been interpreted as basal to slope sediments sharing many of the characteristics of carbonate turbidites as well as deep water environments (Cook and Corboy,

2002; Wilson, 1969). Ettner (1989) described several ichnofossils in the Tuscarora Mountains, which interpret bathymetry and paleoecological conditions during the sedimentation of the DSrm. Mullens (1980), based on the presence of pyrite, carbonaceous material, and absence of fossils hypothesized that during the deposition of the silty limestone that the pH was about 7.9–8.2 and the Eh was close to –0.3. Conodont data near



the Carlin mine indicates an episodic temperature spike between 350–450 °C (Armstrong and others, 1987) that may be related to the intrusion of the Eocene Welches Canyon stock.

At Chukar Footwall (Fig. 3), as elsewhere in the Carlin trend, the SDrm has been divided in four gradational informal units (Sagar, 2000a, 2002b; Harlan and others, 2002). The basal unit, SDrm4, is 220 m of monotonous, planar, silty limestone similar to the upper unit SDrm1.

Samples from this unit only come from deep cores that did not intercept the underlying Ordovician Hanson Creek Formation, the ore host of the Murray mine in the Jerritt Canyon district (Hutcherson, 2002). The SDrm3, with an approximate thickness of about 66 m, is a silty limestone unit easily recognizable due to the presence of quasi-rhythmic centimetric calcarenites beds. The next 52 m, SDrm2 (Fig. 3), consists of a silty limestone with erratic, thin calcarenites beds with laminae to locally wispy textures. Brassy or sooty pyrite is commonly found along or around the wisps and/or zones of carbonaceous matter. The wispy textures have generally been thought of as a product of bioturbation (Armstrong and others, 1998). The upper unit, DSrm1, is 27 m of monotonous silty limestone with some erratic calcarenite beds toward the base.

The medium-dark grey to light grey colors of these units appear to be the result of the degree of hydrothermal alteration, content of carbon, and bleaching by ground waters. Several sedimentary structures have been recognized during underground mapping and from core logging. Load cast structures are somewhat common on the calcarenite beds and can be followed for a few meters until they pinch out with the silty limestone. Also, small sedimentary boudinage, diagenetic structures formed due to the degree of sediment competency during compaction, were noted in a calcarenite bed near the hinge line of the Chukar anticline. The presence of minute flute marks on the sole of the SDrm2 unit (4680 AXS level) records turbidity current movements to the SW/SSW; however, a paleocurrent analysis was not undertaken due to the scarcity of these types of structures in mine exposures. From cores, soft-sediment deformations are common features presenting a range in thicknesses between a few centimeters up to tens of centimeters. Finally, diagenetic stylolites are sub-parallel to the beds with square and irregular waveforms. Dark insoluble residue along the stylolites can be seen at high magnification. In zones of strong decarbonatization, stylolites developed sub-parallel to bedding at both microscopic and macroscopic scales. Two stylolites forms have been observed in hand samples, square and irregular, with a thickness of about 1mm filled with both carbonaceous matter and calcite.

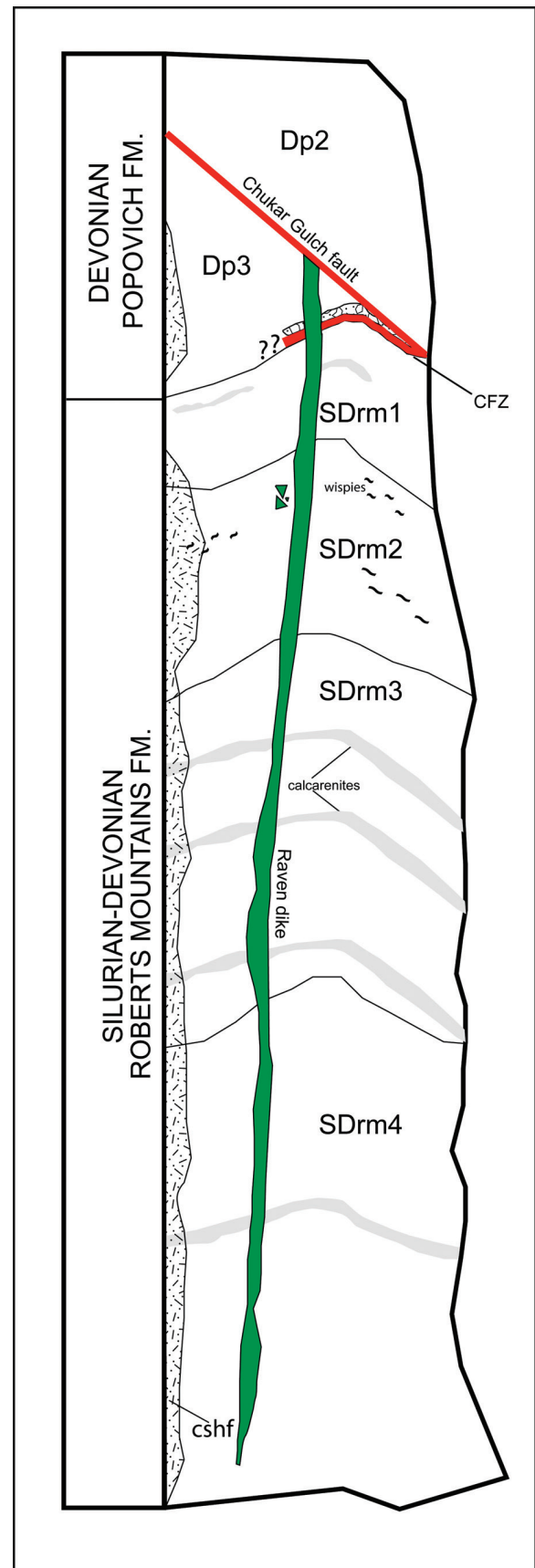


Figure 3. Generalized tectono-stratigraphic section of the Chukar Footwall mine. The contact between the Silurian-Devonian Roberts Mountains Fm. (SDrm1) and Devonian Popovich Fm. (Dp3) is along the Contact Fault Zone (CFZ), a ENE-striking structure. The Raven dike cuts the stratigraphy, and it has been locally brecciated due to later fault reactivation. Thermal metamorphism, that increases to the SW, is characterized by pyroxene hornfels (cshf) that overprint the original carbonate mineralogy.

### **Devonian Popovich Formation**

Structurally overlying the SDrm Formation is the Devonian Popovich Formation (Dp), where only the lower section (Dp3) can be characterized in 3 mine levels. Along the Carlin trend, this formation exhibits different facies attributes and thicknesses as a result of the environments of deposition and later diagenetic processes. Furthermore, the boundary between DSrm and Dp units is in dispute (Evans, 1980; Radtke, 1985; Ettner, 1989; Armstrong and others, 1998; Harlan and others, 2002; Mariño, 2003). Regarding the age of Dp, an Early Devonian-Late Devonian interval has been assumed by Evans (1980), Ettner (1989), and Armstrong and others (1998), whereas Cook and Corboy (2004, Fig. 2) place this formation in the Middle Devonian.

Ettner (1989) reported sections between 210 m at Tuscarora Spur and 70 m in the Carlin mine. Harlan and others (2002) divided this formation into three informal gradational units at Gold Quarry mine, with a thickness of 360 m. The basal units, Dp3, consist of micrites with beds of silty limestone, calcarenite and bioclastic limestone. The overlying Devonian units consist of a thin succession of calcarenites, bioclastites, and silty limestone (Dp2) and brecciated silty limestone (Dp1).

As mentioned above, at Chukar Footwall the contact between SDrm unit and the Dp3 is along the Contact Fault Zone, a northeast trending low angle structure that caps gold mineralization. As identified from cores and mine exposures, the Dp3 is a monotonous package of massive, dark to grey micrites with abundant carbonaceous material, pyrite and calcite veins. Also, the unit is further characterized by zones of crackle-to-matrix supported breccias and local shearing obliterating the rock fabric.

The Dp3 does not host economic grade mineralization at Chukar Footwall mine (Joe Sagar, personal communication, 2004).

### **Breccia bodies**

Breccias bodies are ubiquitous features in the Carlin trend, but their nature and interpretation within the deposit stratigraphy and their relationship with gold deposition have not been conceptualized until recent years, even though such bodies host the main mineralization at the Meikle, Deep Star, Post, and Rain deposits (Emsbo and others, 2003; Heitt and others, 2003; Williams, 1992). At the Gold Quarry mine, Williams (1992) described collapse and fault breccias. Texturally, the collapse breccias consist of angular monolithic clasts of the SDrm in a matrix of calcite, barite, and quartz. Breccias geometries range from funnel to tabular to irregular shapes, and are spatially related with decalcified rocks. Geochemically, these bodies are enriched in Au, As, Hg, and Sb relative to the surrounding SDrm units. With respect to fault breccias, this author characterized both NNE and NNW trending structures displaying fragment zoning and tabular geometries. These structures record several episodes of brecciation, minerals deposition, and element enrichment which indicate they were feeder structures (Williams, 1992).

The contact between the SDrm Fm. and the Dp Fm. is characterized by a high fracture and fault density zone, breccia bodies, and calcite veins along both the footwall and hanging-wall of the Contact Fault Zone (CFZ). Breccia types recognized along the contact (e.g., in the 4610 level and Tracker Decline) include a component of fault breccias, angular to subangular fragments of limestone strongly decarbonatized and silicified, whose structural fabric has been somewhat obliterated by later hydrothermal alteration events and fault reactivation(s). Strong decarbonatization resulted in the collapsing of the section by carbonate removal, which was channalized along the hanging-wall section of the fault with resultant formation of dissolution collapse breccias and a dense calcite stockwork. A key component is a sub-parallel, metric tabular body of dissolution collapse breccias along the hangingwall of the CFZ. The breccias consist of angular, poorly sorted limestone fragments exhibiting a range of sizes, crosscut by late calcite veinlets. The matrix is a vuggy, wavy-banded calcite (neither ferroan calcite nor ferroan dolomite was identified during carbonate staining). Although pervasive, late silicification varies from weak to strong along the section. Provisionally, the formation of the dissolution collapse breccias was a pre-ore event that acted as a stratigraphic cap for later hydrothermal, gold enriched fluids (Joe Sagar, personal communication, 2004).

In the SDrm breccias are a common feature, especially in the SDrm1–2 units. In the Dp3 unit, however, brecciation is much less pervasive than in the underlying units due to the massive fabric of the micrites and/or lower concentration of fractures and joints channeling fluids responsible for the chemical dissolution of the rocks.

Collapse breccia bodies have been recognized in the 4610 and Tracker Exploration Drift mine levels. One such body is a vertical, funnel shape of about 4 m high and 2 m wide composed of poorly sorted, angular monolithic clasts ranging from millimeter to several centimeters in size and consisting of decarbonatized and silicified SDrm1 embedded in a calcite matrix. Internal sedimentary structures are absent; however, there is a crude orientation of the clasts' long axes that may be interpreted as being parallel to former bedding planes. The fragment orientation appears to be the result of in-situ brecciation. The spatial position of this breccia body relative to a NNW-trending fault zone supports the interpretation that the structure served as a pathway for hydrothermal fluids. Briefly, the breccia sample shows enrichment in Au, Ag, As, Sb, and Ti; and depletion in Ba, Cr, and Mg relative to the limestone.

### **Intrusive rocks: The Raven Dike**

A wide variety of dikes have been reported in the Carlin trend, including lamprophyre, monzonite porphyry, latite, dacite, rhyolite, and granodiorite to diorite (Radtke, 1985; McComb, 1993; Altamirano, 1999; Tretbar, 2000; Chakurian, 2001; Jackson and others, 2002; Heitt and others, 2003; Mariño, 2003). Available radiometric data suggest at least two main peaks of intrusive activity related with both the emplacement of the Gold-

strike stock at about 159 Ma, and the Richmond stock at 106 Ma (Evans, 1980; Moore, 2001; Norby and Orobona, 2002). Similarly, Evans (1980) reported a radiometric age of 37 Ma for a small quartz monzonite intrusion, the Welches Canyon stock, and related dikes in the Lynn window. Dikes are mainly characterized by (1) emplacement along high angle structures with sharp contacts, (2) host economic gold mineralization (e.g. the Beast dike, Ressel and others, 2000), and (3) extensive hydrothermal alteration that makes it difficult or impossible to determine the original fabric and geochemistry in most cases.

Several NNW-trending latite dikes have been exposed in the Gold Quarry pit showing a high degree of alteration (McComb, 1993). Although no age constraints exist yet, these dikes have been tentatively assigned to be Jurassic-Cretaceous in age in Newmont's cartography, and they pre-date the main gold mineralization period (Harlan and others, 2002). In addition to these dikes, there is a prominent intrusion known as the Raven dike exposed in several underground levels in Chukar Footwall. Dike emplacement was along NW-to-NNW trending structures, with steeply bimodal dips. The Raven dike has been slightly offset and rotated by some NE-trending structures (e.g., Magpie fault). It shows local intense brecciation toward the borders due to later fault reactivation.

The Raven dike shows sharp contacts with the SDr<sub>m</sub> and Dp units, producing a visible, metric scale thermal effect on either side characterized by an intense rock bleaching and recrystallization of carbonates. The dike ranges from a few centimeters up to a meter in width, and up to 220 m in length at the 4650 level (Newmont, 2003). Furthermore, the dike may locally be mineralized (Joe Sagar, personal communication, 2004).

At outcrop scale, the dike is easily recognizable by its greenish, gummy clay that produces a perceptible, irregular alteration halo. Although the dike is completely altered, it shows a very homogeneous texture. In thin-sections (Fig. 4), the dike is characterized by gross inequigranular, glomeroporphyritic textures of relic phenocrysts of feldspars, pyroxenes, and biotite in a fine groundmass totally altered to sericite, kaolinite, anhydrite, quartz, and unidentified opaques. Plagioclase is totally altered to microcrystalline masses of sericite, quartz, and kaolinite. Similarly, biotite is replaced by iridescent sericite and chlorite. Sulfide minerals, pyrite and marcasite, comprise up to 10 vol. % of the rock and they partially or completely pseudomorph mafic phenocrysts. Pyrite, the main sulfide mineral, occurs as anhedral to subhedral grains locally replacing mafic phases, forming late veinlets, and in discrete grains overgrown by marcasite. From deep hole samples (QRC1489-1040'), there is an observable density increase in pyrite veinlets, altered to malachite, relative to samples from mine exposures. Late barite and fluorite veins crosscut the dike. Anhedral to euhedral discrete purple fluorite grains are distributed along barite cleavages and fractures, and fluid inclusions are abundant. Finally, prismatic apatite phenocrysts were observed within the dike groundmass without any indication of alteration.

The above petrographic description, coupled with data by McComb (1993), indicates the Raven dike appears to be either a lathy-latite or a porphyritic monzonite showing an advance degree of hydrothermal alteration (quartz-kaolinite-sericite-pyrite).

### Structural outline of the Chukar Footwall Deposit

The current structural settings of the Gold Quarry-Chukar Footwall deposits are a direct consequence of the tectonic events since the Antler orogeny. Cress (1972) recognized four tectonic phases in the Carlin-Maggie Creek window producing shallow plunging, NE- to NW-trending mesoscopic folds. These range from open to tight folded structures. Reverse NW-striking faults and normal NW- to NE-striking faults are the dominant fault trends and styles. Similarly, Cole (1995) established four episodes of faulting at Gold Quarry: (1) folds related to the Roberts Mountains allochthon thrusting, (2) events of wrench, reverse, and normal faulting, (3) normal faulting due to collapse during decarbonatization, and (4) normal faulting during the Tertiary extensional regime.

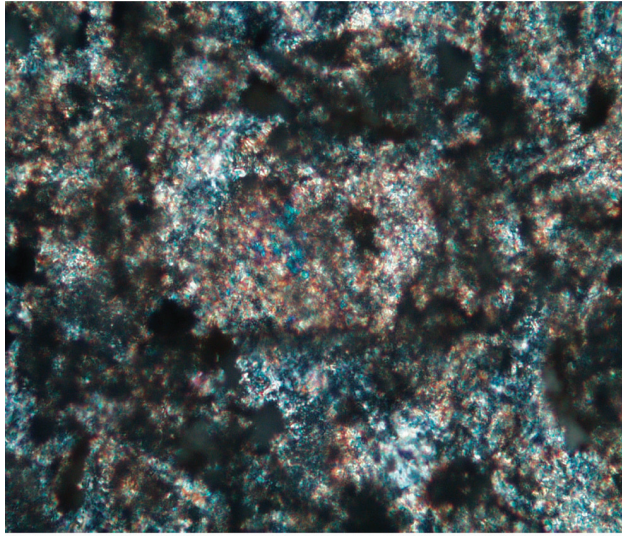
The structural history of the Chukar Footwall mine is outlined in Table 1. Gold mineralization was strongly controlled by major and minor structures. The more important ore-controlling feature is the structural intersection of the Chukar anticline with northeastern structures (Joe Sagar and Kevin Creel, personal communication, 2005). On the other hand, minor structures (fractures and joints) are of great importance in controlling and localizing gold pods by increasing the amount of open space in the host rocks whereby the ore fluids were able to move farther, both vertically and horizontally from major fluid conduits.

### Folding and faulting

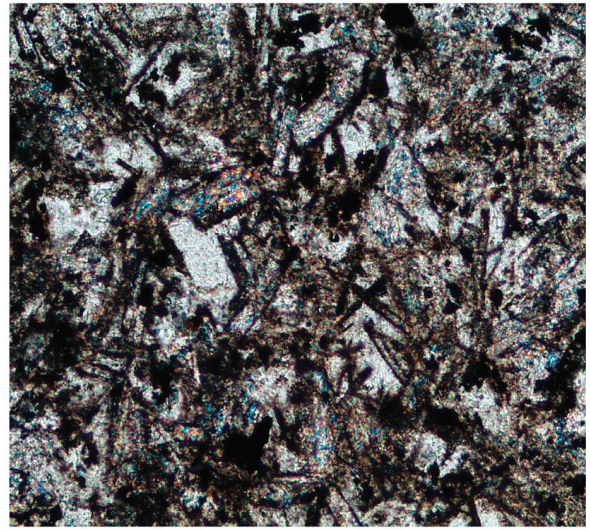
The Chukar anticline is the main macroscopic features observable underground (Fig. 2). This structure, at outcrop scale, does not exhibit any penetrative fabrics within the thin-to-massive bedded silty SDr<sub>m</sub> units nor in the Dp3 lithologies. Adjacent and subparallel to the NE-striking Chukar Gulch fault, the Chukar anticline (Fig. 5B and 6) is a northeast-trending open structure that plunges at shallow angles to the SSW (217°/2° SW). Small scale parasitic folds are present in the northwest and southeast limbs of the anticline, with axes trending WNW and NE, plunging 10° and 14°, respectively. The Chukar anticline has been offset up to 22 m by the Sagehen fault, a NW-trending structure (Joe Sagar, personal communication, 2005), and bedding attitudes in both limbs indicate an asymmetric, non-cylindrical structure because all the poles are not homogeneously distributed along a great circle (fig. 5B). The anticline is a fairly simple structure, with bedding thickness at the hinge zone up to 1 m and thin limbs of about 14 cm in thickness typical of similar folds (Ramsay and Hubert, 1987).

Brittle deformation is represented by two dominant fault trends throughout the deposit (Figs. 2 and 5A): (1) a WNW/NNW-trending system represented by major structures

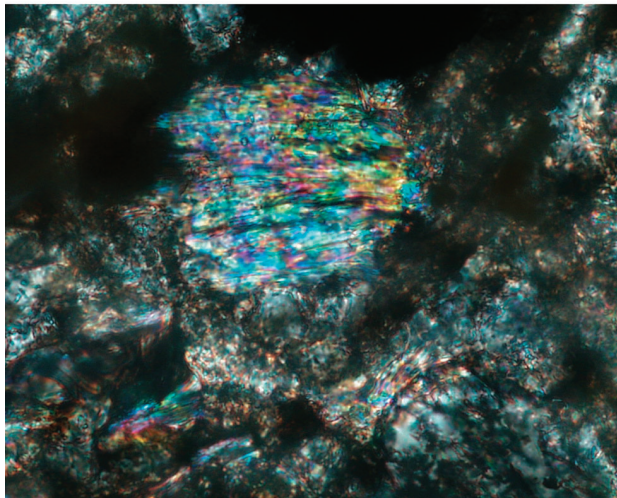




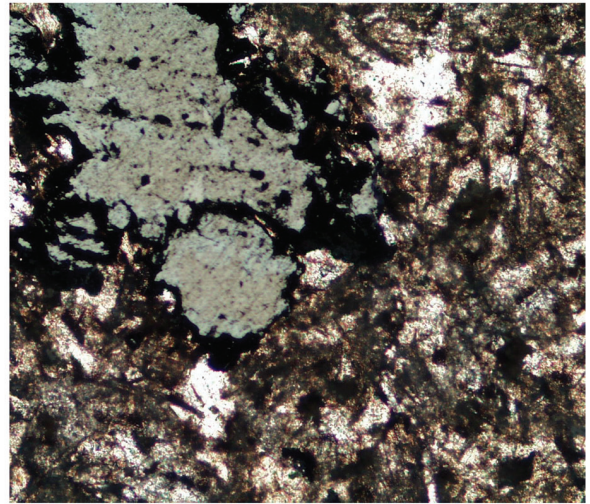
1



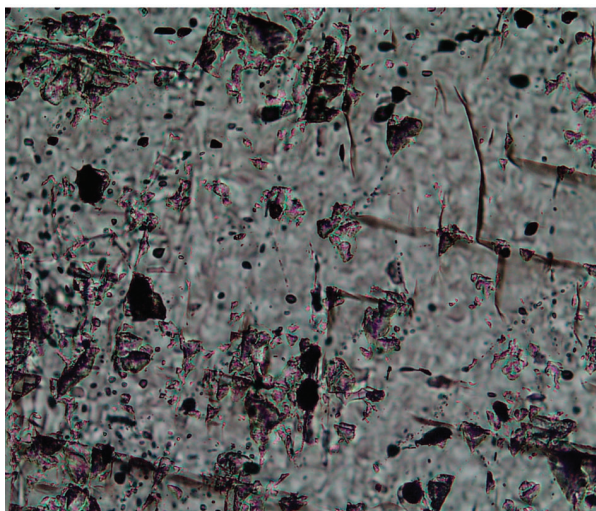
2



3



4

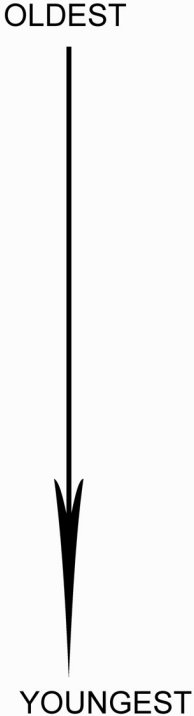


5

Figure 4. Photomicrographs of the Raven dike, an altered lathy latite. Crossed nicols (1,2,3,and 5) and reflected light (4). (1)Mafic phenocryst totally altered to a fine quartz-kaolinite-sericite mass. Dark, brownish leucoxene forms peripheral alteration clouds around coarse phenocrysts (FOV: 0.21 mm). (2)Intense quartz-kaolinite-sericite-carbonate alteration of both the medium-grained mafics and feldspar phenocrysts and the fine-grained groundmass. The dark tabular phenocrysts randomly distributed in the groundmass are argillized and sericitized plagioclase laths (FOV: 0.43 mm). (3) Chlorite replacement of biotite (FOV: 0.21 mm). (4)Anhedronal to subhedronal pyrite grains rimming and sulfidizing mafic phenocryst (FOV: 0.21 mm). (5) Late barite-fluorite vein. Triangular pits of fluorite along cracks or cleavages of earlier barite. Fluorite contains fluid inclusions. (FOV: 0.21 mm).



TABLE 1. PRELIMINARY STRUCTURAL PARAGENESIS AT CHUKAR FOOTWALL MINE

	Chukar anticline	NE37E/2 SW, Antler orogeny
	E-W/65 S	Pre-ore structures?
	N70E/SE+N36E/SE+CFZ	Carbonates+silica+As and Sb minerals. Feeder structures
	Contact metamorphism	37 Ma ( Welches Canyon stock) Pyroxene hornfels.
	N310E/NE+ Raven dike	Carbonates+barite. Dike altered to QSP
	Gold mineralization	Eocene. Strong decalcification+ qtz+ser+dolo+py+barite
	Reactivation of structures	Late Tertiary extension

such as the Jay, Pheasant, Antelope, Sagehen, Raven Dike, Mallard, and Crow faults, and (2) NNE-NE trending faults represented by the Contact Fault Zone (CFZ), Magpie, and Chukar Gulch faults. Both fault systems record, at least, two sets of slip indicators due to later fault reactivation thus producing incoherent crosscutting relationships.

The WNW/NNW-striking fault system commonly has both moderate and steep dips to the NW and to the SE (Fig. 5A). In general, they are structures up to 2 meter wide, with gummy clay and brecciated, friable gouge. Kinematics indicators such as calcite crystal fibers, grain striations, and fault mullions point out multiple senses of displacements in both fault systems due to later reactivation(s). Sub-horizontal to sub-vertical rakes were recorded on fault planes discerning a general trend of (1) an oblique dextral normal slip, which rakes between 10 to 60 degrees to the northwest, and (2) strike-slip faults with sub-horizontal slickenlines. The Raven dike was emplaced along NNW-trending structures (e.g. Raven Dike fault at the 4580 and 4590 levels), and seems to be synchronous with the development of these fractures based on the sharp contacts. This fault system is post-ore; however, a stable isotopic transect and gold values perpendicular to the Antelope fault at the 4740 level may suggest a post-ore mobilization of elements in the hangingwall section.

The conjugate of the WNW-NNW faults is a system of NNE/NE-trending faults, which are cut and offset by the former

structures. These faults are predominantly high angle, with steep NE and SW dips (Fig. 5A). These faults are characterized by a brecciated, wellhealed gouge with locally abundant rock flour and late calcite±barite veins. The Magpie fault, the main feeder structure at Chukar Footwall, hosts a discontinuous calcite ± barite ± stibnite breccia zone along dilation jogs. Stibnite deposition postdates movements on the structure due to lack of crystal deformation. Late stage fracture controlled minerals include orpiment, realgar, and barite. The CFZ is being interpreted here as a low-angle normal fault zone (a thrust?), with sigmoidal minor, subparallel structures. The dip of the CFZ fluctuates between 55° and 30° toward the southeast; it separates the Popovich Fm. in the hangingwall from the Roberts Mountains Fm. in the footwall. It is regarded as an ore-controlling feature that caps gold mineralization at Chukar Footwall (Joe Sagar, personal communication, 2004). Slickensides measured along this fault zone rake 47° to 55° to the southeast. The main characteristic of the CFZ is the continuous presence in the hangingwall section of an apron of fault and collapse breccias, and a dense stockwork of calcite veins. The CFZ contains little gouge and is locally coated with carbonates and red clays. The extent of this fault zone is still unknown as is illustrated in Figures 2 and 6; however, the apron-like map view of the fault and collapse breccias may favor an arcuate, convex geometry for the fault trending southwest with the fault flattening at depth. Alter-

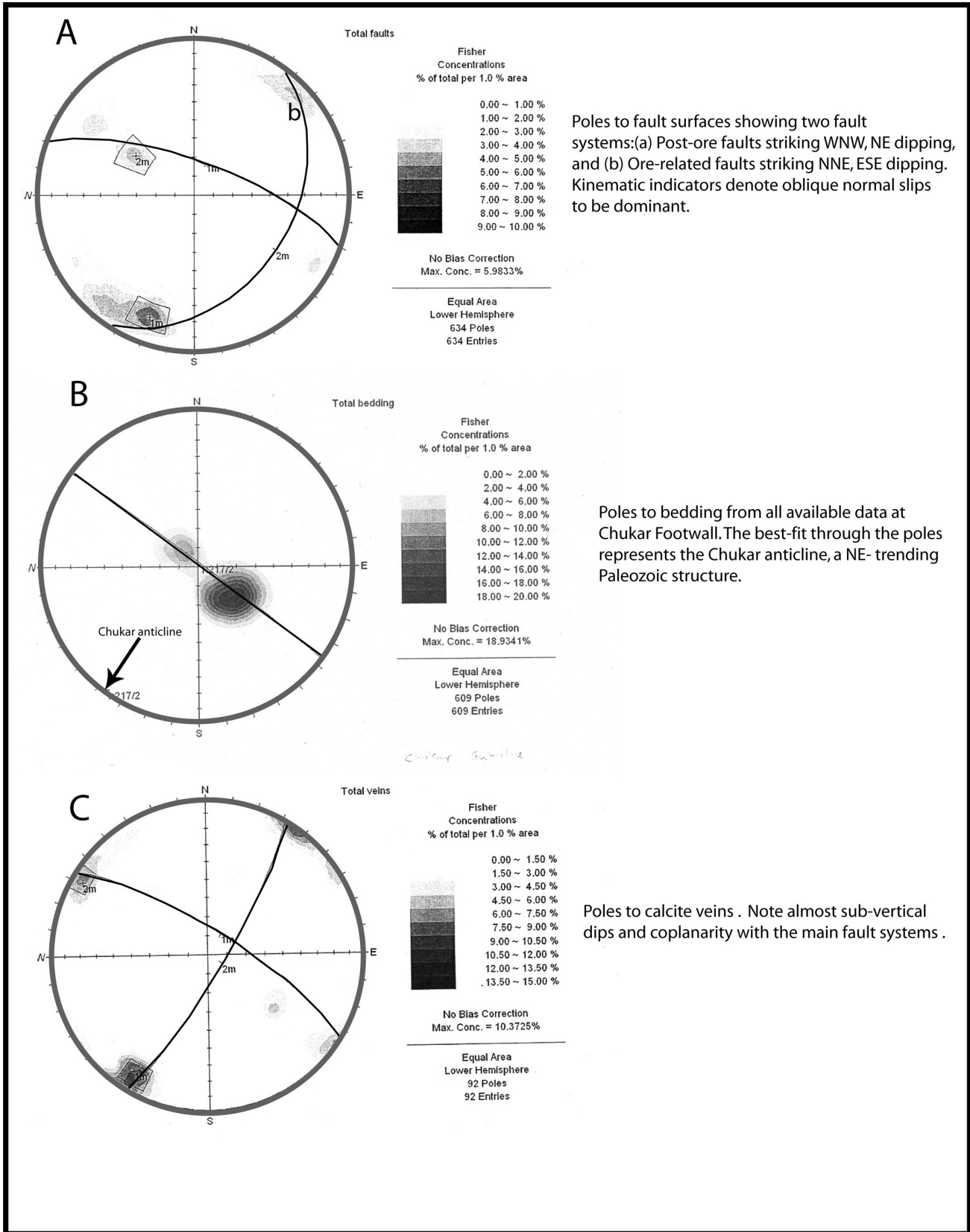


Figure 5. Stereoplots of poles to fault planes (A), poles to bedding (B), and poles to calcite veins (C) at Chukar Footwall mine. Data from all levels (database from Newmont and this project).

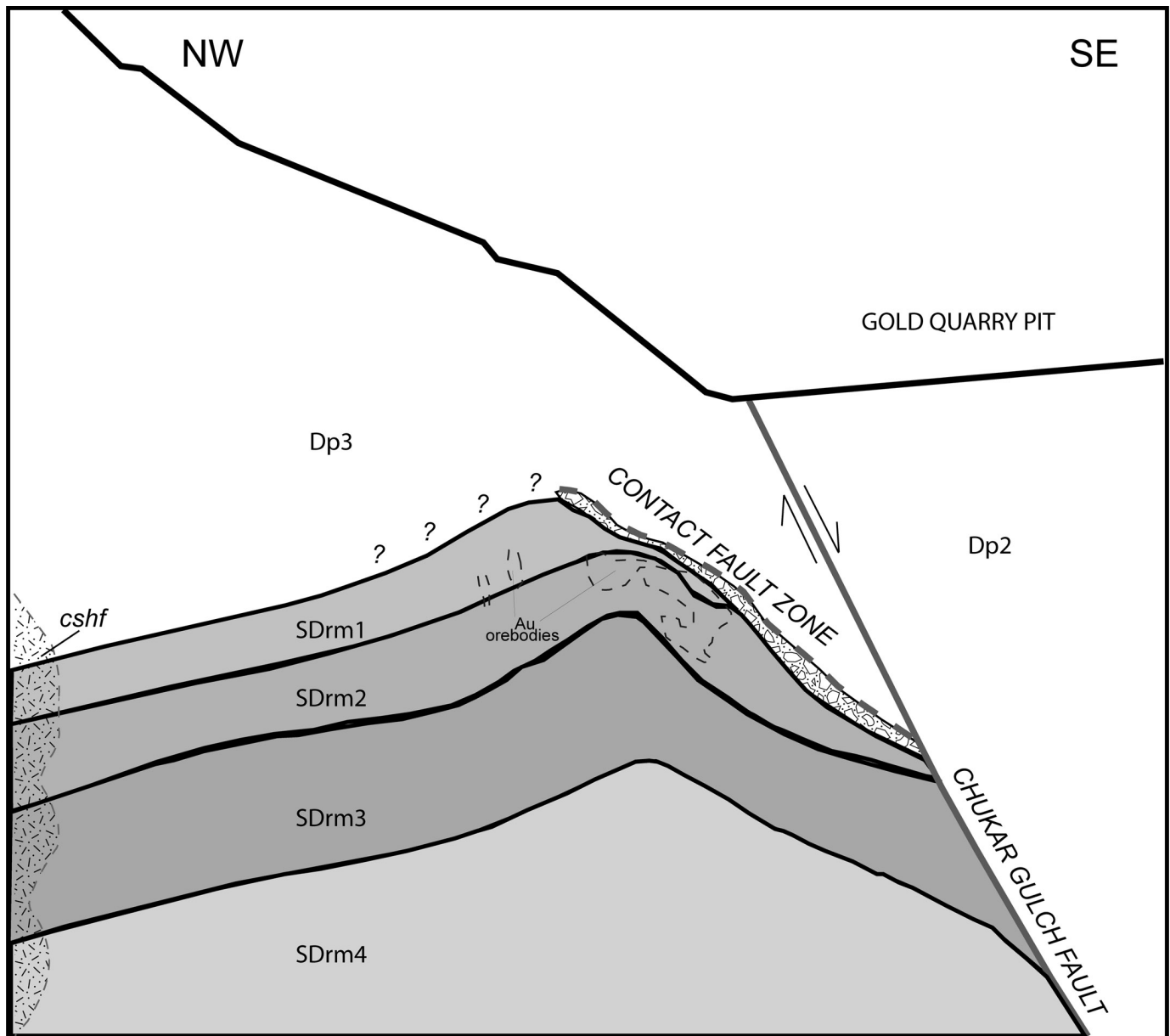


Figure 6. NW-SE cross section of the Chukar deposit. The Chukar anticline (N37/2 SW) is the earliest structure within the deposit that may be related to the mid-Paleozoic Antler orogeny. Stratabound, high grade gold mineralization is mainly concentrated near the fold hinge. The Contact Fault Zone is interpreted as a ore fluid trap. The main control to gold mineralization is the structural intersection between NE-striking structures (i.e., Magpie fault) and the anticline (Modified from Newmont, 2003).

natively, the breccias may have formed entirely by dissolution and collapse processes that localized later fault development (Tommy Thompson, personal communication, 2005).

Structures similar to these at Chukar Footwall have been describe along the Carlin trend (cf. Evans, 1980; Lewis, 2001); thus, the relative timing of folding and faulting can be somewhat constrained. The NE-trending Chukar anticline is difficult to interpret compared to the general NW-trending anticlinal fold suites along the Carlin trend. Evans (1980) describes similar trending folds in the Lynn Window as a result of horizontal

compressional forces onto lower plate rocks due to the eastward to southeastward emplacement of the Roberts Mountains allochthon during the Antler orogeny. The WSW-ENE compressional stresses developed during the Sonoma orogeny were responsible for the development of multiscale regional anticlines oriented NNW such as the Post and Tuscarora anticlines (Mariño, 2003; Lewis, 2001). Finally, four main episodes of faulting have been distinguished within the Chukar Footwall deposit based on crosscutting relationships, from older to younger (Fig. 7, Table 1): (1) ENE-striking faults, (2) NE-striking faults,

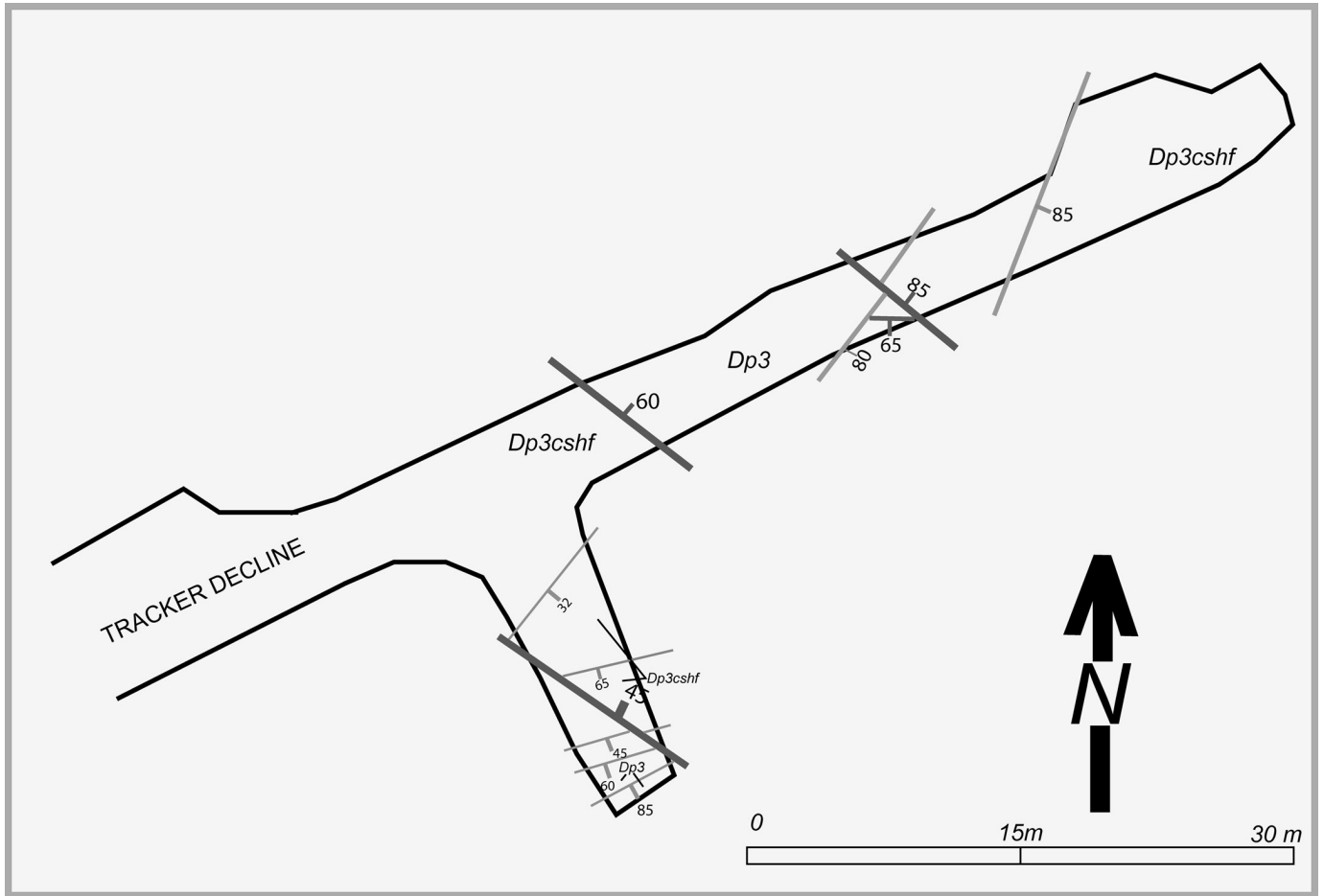


Figure 7. Crosscutting relationships among sets of faults at the Tracker Decline. Most of the NW-striking faults cut and offset older NE-striking faults. However, Cenozoic extension fault reactivation was widespread thus producing contradictory crosscutting relationships and extensive brecciation. Symbols are the same as on Figure 6.

(3) NW-striking faults, and (4) reactivation of older structures due to the Tertiary extensional regime (cf. Lewis, 2001). Later extensional faulting reactivated older faults generating oblique slips, particularly on the NW-trending structures (Fig. 8).

## GEOCHEMICAL DATA

The geochemical data comes from 53 samples collected during underground mapping and from a data set of mineralized intervals provided by Newmont. Samples were analyzed for multi-elements by ICPMS at Newmont. The selected samples were taken perpendicular to and at measured intervals from structures such as faults, joints, and veins to determine possible ore fluid pathways and to make geochemical comparisons between mine levels. Also, the geochemical data have been utilized in identifying hydrothermal alteration signatures. Two correlation matrices of elements were produced to contrast the geochemical signature distributions between the entire deposit and selected mineralized intervals within the deposit.

As outlined by Craig and Wakefield (1991) and Rota (1991), the geochemical signature of the Carlin trend and the Gold Quarry mine are generally depicted by a gold suite of elements (Au-As-Sb-Hg-Tl) and a base metal suite (Ag-Cd-Cu-Pb-Zn), which have been interpreted to represent several synkinematic deposit-scale metal mobilizations from the host rock lithologies into structures (Sha, 1993).

Geochemical data from the Chukar Footwall deposit show some differences compared to those described for the Carlin trend. At the deposit scale, Au correlates weakly with As, Co, Cu, Fe, Hg, and Te. Ba and Sb, reflected in the ore mineralogy as barite and stibnite, show no correlation with Au. This observation, tentatively, may be explained by their post-ore nature among Carlin-type deposits (Harris and Radtke, 1976; Sha, 1993; Arehart, 1996; Heitt and Dunbar, 2003; Mariño, 2003). On the basis of their strong correlation ( $r \geq 0.700$ ), four correlative elements suites are represented at entire deposit scale by the association of (i) As-Hg, (ii) Bi-Sn-Te, (iii) Ca-Zn, and (iv) Li-Ti. However, the geochemical signature of high gold grade



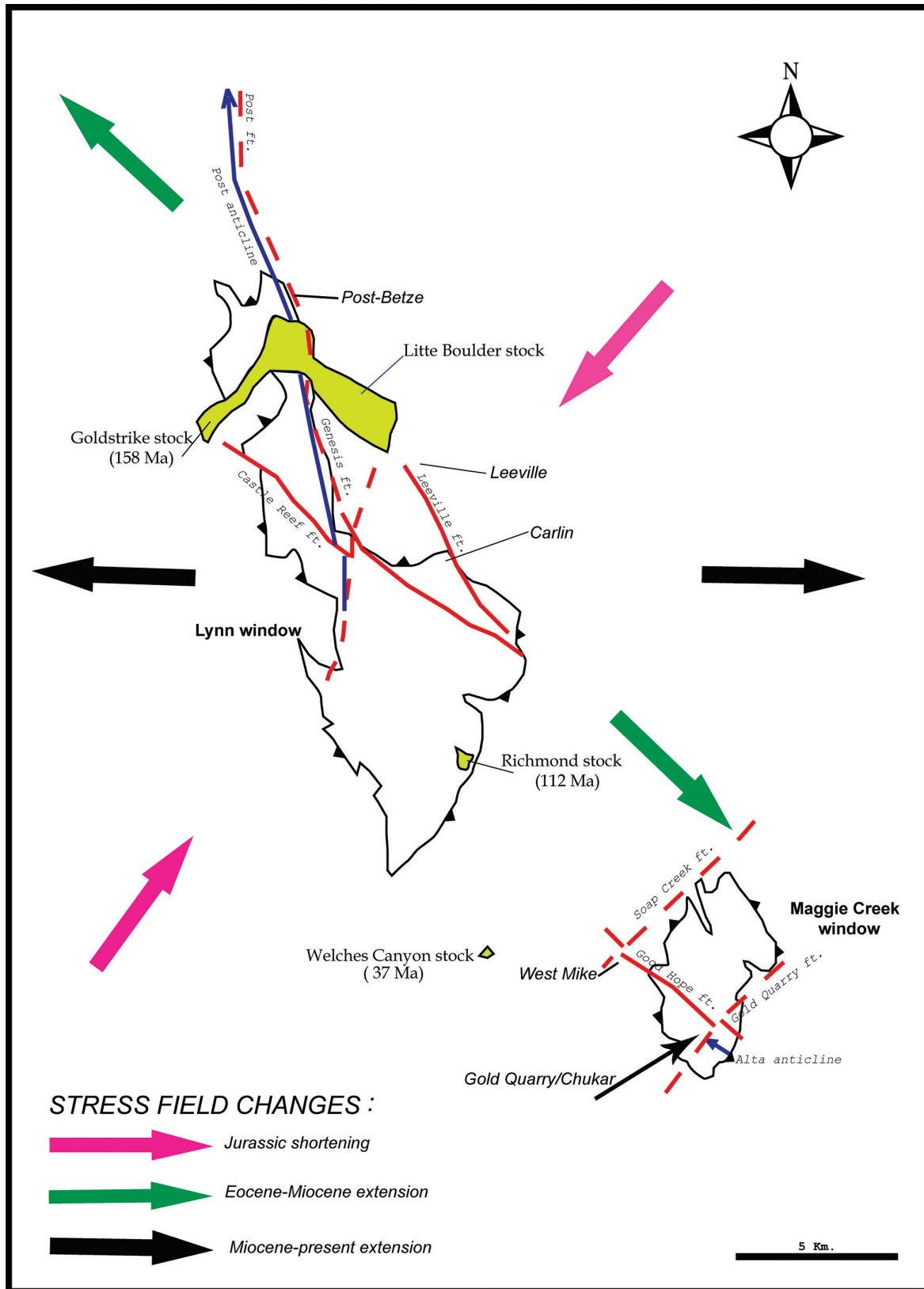


Figure 8. Geological framework of the north and south areas of the Carlin trend showing the Lynn and Maggie Creek-Carlin windows, which host gold mineralization of Eocene age. Main stress fields, denoted by colored arrows, record significant Jurassic compression, and Tertiary multi-phase extensional regime with probable fault reactivations (modified from Moore, 2001; Lewis, 2001).

intervals shows that Au correlates well ( $r \geq 0.600$ ) with Co-Cu-Ni-Tl, and As and Te correlate weakly with gold ( $r \geq 0.400$ ). Data from the high grade samples show a general enrichment in Al, As, Cr, Cu, Fe, Sb, Hg, Pb, Ti, and Tl and a depletion in Ba, Ca, Sr, Mo, and Zn relative to low grade-unmineralized samples. Finally, a systematic incompatible behavior pattern between Al and Ba has been noticed: as Al increases/decreases, Ba decreases/increases.

The results of the geochemical distribution of some selected elements (As, Ba, Fe, Sb, and Tl) within the entire deposit show an overall random behavior; however, the spatial distribution of elements appears to form a continuum reflecting the influence of host rock lithology, the degree of wallrock alteration, and their relative proximity to structures. First, the SDRm rocks have heterogeneous geochemical features as is reflected by their gradational lithologies, diagenetic histories, and effects from thermal events thus introducing random or unclear geochemical distribution patterns. Second, the results of hydrothermal alteration across structures show a tabular zonation of elements. For example, transect data perpendicular to the Maggie fault on the 4720 level indicate a strong concentration of Au, As, Fe, and Sb close to the structure; away from the fault a sharp decrease in these elements, accompanied by an increase in Zn, and erratic behavior of Ba characterize tabular geochemical zonation (Fig. 10).

In summary, the geochemical signatures of the Chukar Footwall deposit are characterized by a correlative suite of Au-Co-Cu-Ni-Tl and an irregular distribution of elements within the entire deposit. However, wallrock alteration and structures are factors controlling tabular, metric-scale element zonation.

## HYDROTHERMAL ALTERATION

The Chukar Footwall mine exhibits hydrothermal alteration assemblages typical of Carlin-type gold deposits: (a) decarbonatization, (b) dolomitization, (c) silicification, and possibly (d) baritization and oxidation of iron sulfides. Aehart (1996) evaluated the hydrothermal alteration in the Carlin trend and concludes a general spatial pattern of wallrock alteration that can be characterized by distal, volumetrically extensive decarbonatization that envelopes silicified and argillized zones adjacent to the gold mineralization. With regard to temporal relationships between these alteration types, recent work by Harlan and others (2002) summarized wallrock alteration paragenesis in the Maggie Creek district typified, from oldest to youngest, by decalcification  $\rightarrow$  dolomitization-sericitization  $\rightarrow$  silicification  $\rightarrow$  argillization  $\rightarrow$  sulfidation  $\rightarrow$  supergene weathering.

At Chukar Footwall, the hydrothermal alteration was initiated by a decarbonatization event(s) along faults, faults zones, joints, and along bedding planes. Such structures fully control the extent of decalcification producing sharp boundaries between altered and fresh rocks, a distinctive trademark of this deposit relative to the Carlin mine (Mike Robinson, personal communication, 2004). The degree of decarbonatization is

accompanied by variations in the amount of calcite veins and stockworks, stylolites, and brecciation. Multistage white calcite veins range from a millimeter up to a meter wide, and they are usually concentrated within the hangingwall of structures and along bedding planes; Figure 5C shows poles to calcite veins, which are coplanar to the two main fault sets in the deposit (Fig. 5A). Another abundant decarbonatization phenomenon is the relative sanding of the silty limestone near major structures. Following decarbonatization, a selective, fracture controlled hydrothermal dolomitization took place within the SDRm and Dp units (Fig 9). The spatial extent of this alteration event is unknown; however, carbonate stained samples document a volumetrically small dolomitization stage on the deposit scale. Transitions from calcite to ferroan calcite to ferroan dolomite are either fracture controlled or selective; typically, the dolomitized rocks are cut by calcite or barite veinlets. District wide dolomitization has been ascribed to form as hydrothermal fluids were focused along major and minor structures diffusing throughout the rocks and producing a dolomitization front of limited extent (e.g. Stenger and others, 1998). Silicification, much easier to detect than dolomitization, represents the third main hydrothermal alteration stage characterized by microcrystalline silica flooding replacing the silty limestones units (jasperoids) and breccias bodies with variable degrees of silica content. Quartz veinlets are common, and they crosscut at a high angle the stratigraphy and earlier calcite veins. Silicification processes are volumetrically important toward the deeper levels of the mine, probably associated with the CFZ and NE-striking structures. Similar precipitation mechanisms responsible for silica precipitation in Gold Quarry was also operating in Chukar Footwall as determined by analogous mineralogical patterns at Gold Quarry characterized by an early microcrystalline silica replacement, followed by barite precipitation in small veinlets (Harlan and others, 2002). Similarly, silicification is structure-controlled, and there is evidence for multistage events of hydrothermal quartz.

The final main stage of alteration is represented by a widespread barite flooding and veining, apparently associated with subparallel NNW marcasite-pyrite and calcite veinlets. What is striking about this late stage is the presence of abundant, visible gold flecks associated with late barite veinlets on the 4730 level. From hand samples, visible gold blebs intergrown with barite, suggesting coprecipitation in a redox condition for such a late phase suite. Briefly, late ore fluids responsible for the deposition of the late gold $\pm$ barite suite were acidic as indicated by the presence of marcasite. The reaction  $2\text{Au}(\text{HS})_2 + \text{Ba}^{2+}_{(\text{aq})} + 2\text{O}_2 \rightarrow 2\text{Au} + \text{BaSO}_4 + \text{H}_2\text{S}$  indicates that Au is reduced while S is oxidized; that is, the chemistry of the late stage ore fluids changed from reducing to oxidizing conditions thus coprecipitating gold and barite. Associated with this late stage, hydrothermal dedolomitization, the replacement of dolomite by calcite, has been reported by Williams (2002) in samples from the 4730 level as calcite incipiently replaces diagenetic or hydrothermal dolomite.

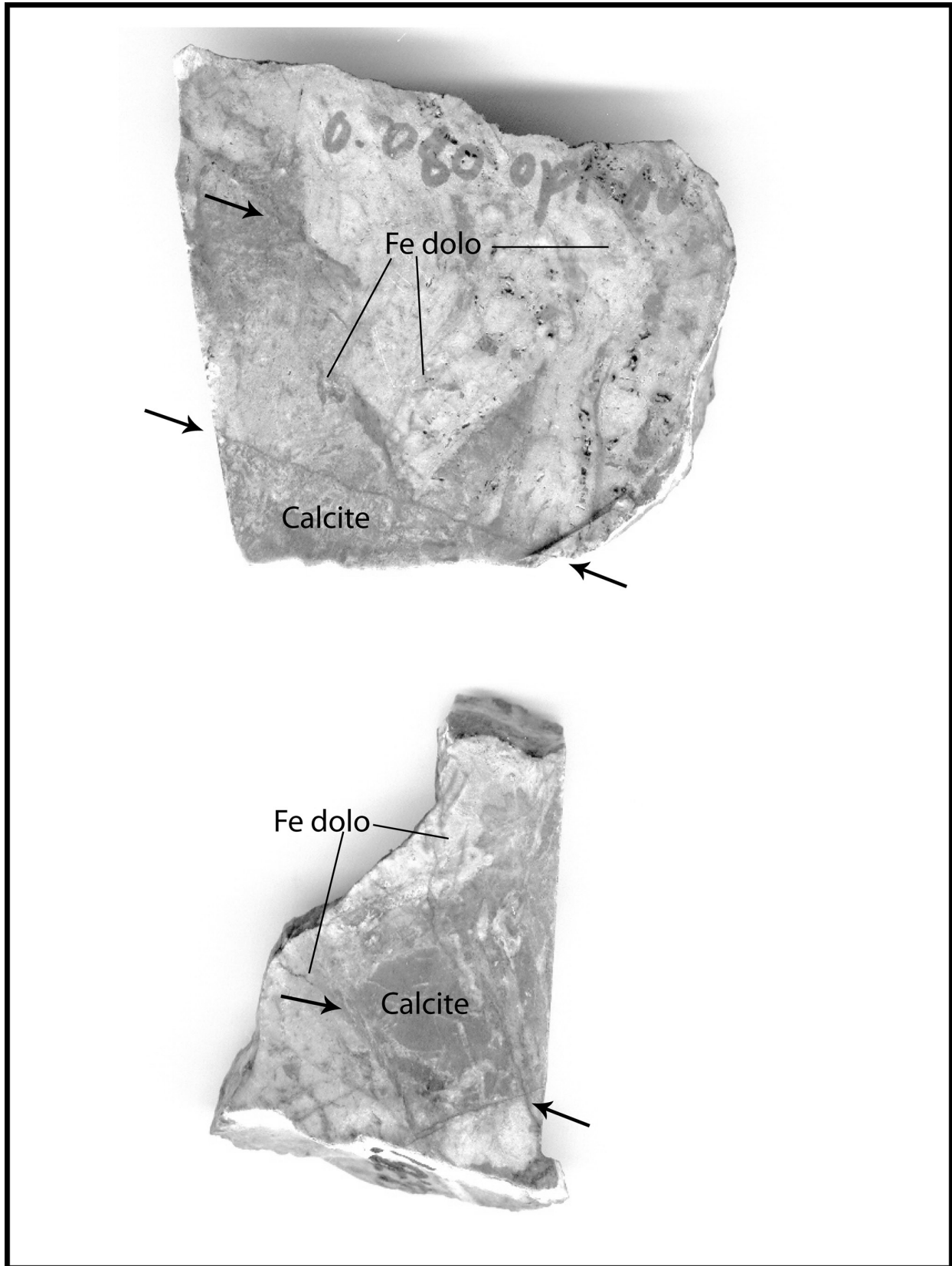


Figure 9. Fracture controlled hydrothermal ferroan dolomite (light color) exhibiting veinlets cutting calcite (dark color). Stained samples from the Tracker Exploration drift, near a high-angle NE-striking structure. Pyrite grains are abundant along and near the fractures (arrows).

## OREBODY FEATURES

The Chukar Footwall mine is currently mined by longhole-stope and cut-and-fill methods. It has produced about 146,000 ounces of gold with an average grade of 0.288 opt Au from unoxidized ore since underground operations began in 1996 (Joe Sagar, written communication, 2005).

The deposit consists of irregular stratabound orebodies within the SDrm units with a strong structural control. Figure 10 shows trace element concentrations with gold grades along a geochemical transect across the NNE-striking Magpie fault at the 4740 level. Decreases in Au, As, Fe, and Sb away from the fault clearly reinforce that the Magpie fault acted as a feeder structure, channeling the hydrothermal fluids toward the

anticline east limb. However, data from a geochemical transect from the CFZ, a low angle ENE-striking structure, revealed erratic, low gold values compared to those adjacent to the Magpie fault; thus, this structure, and possibly all ENE-striking ones, may be considered as barren structures. In addition to this structural control, a grade-thickness map generated by Newmont (2004) (Fig. 12), coupled with Figures 2 and 6, demonstrates that (1) gold orebodies form two main sub-parallel trends running approximately NNE: one along the east limb of the Chukar anticline and one parallel to the Magpie fault; and (2) brittle deformation (e.g., NNE-striking structures and joints and shear fractures) played an important role in focusing ore fluids toward the Chukar anticline hinge and limbs, resulting in the formation of economic orebodies. A regional comparison on

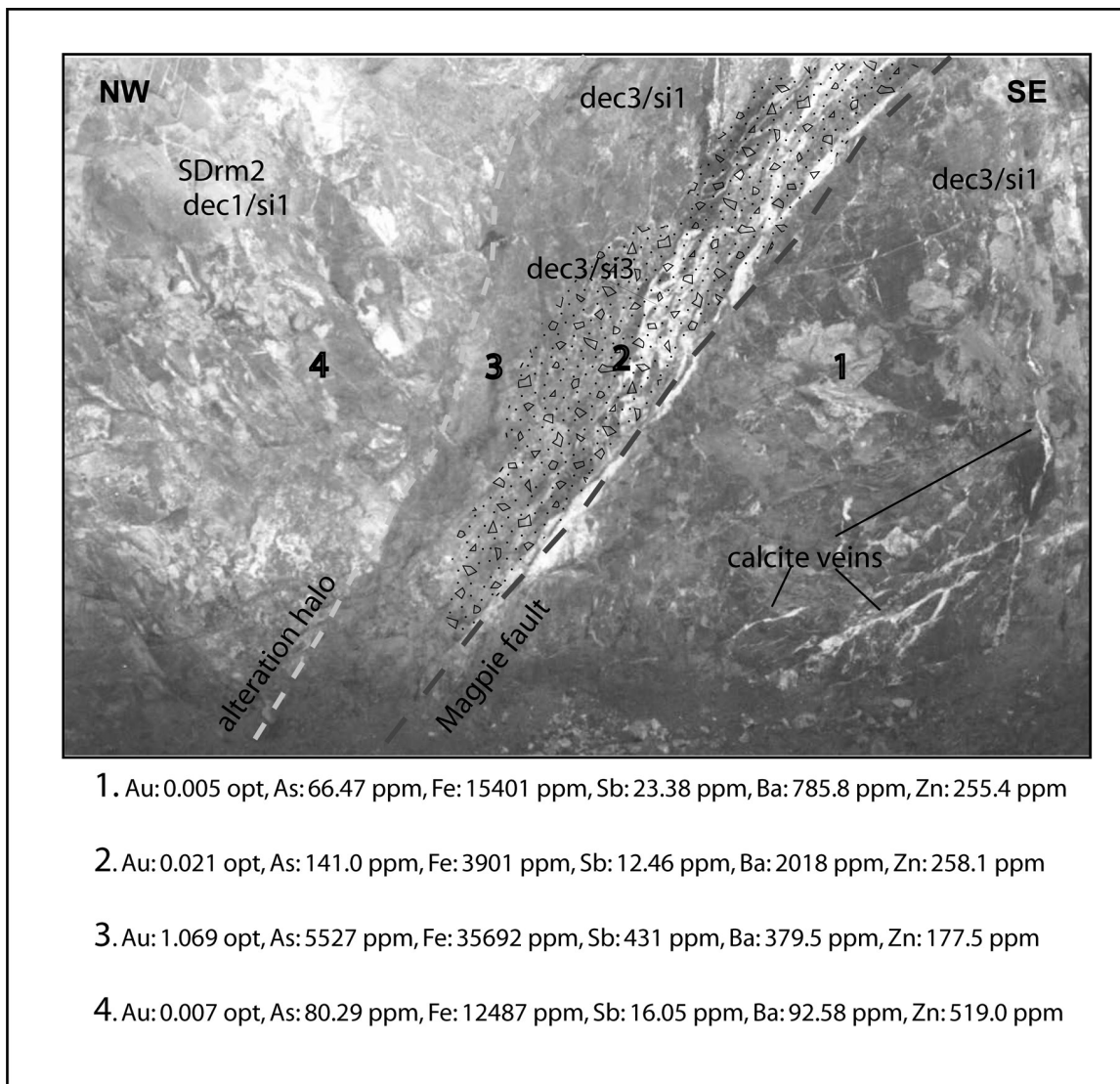


Figure 10. The Magpie fault-vein, a high angle NNE-striking fault, served as a pathway for ore fluids with As, Au, Fe and Sb values decreasing away from the structure. Late, euhedral to subhedral stibnite and barite were deposited in open spaces within the fault breccia (4720 level). Decarbonatization and silicification are coded as weak (dec1, si1) or strong (dc3, si3).



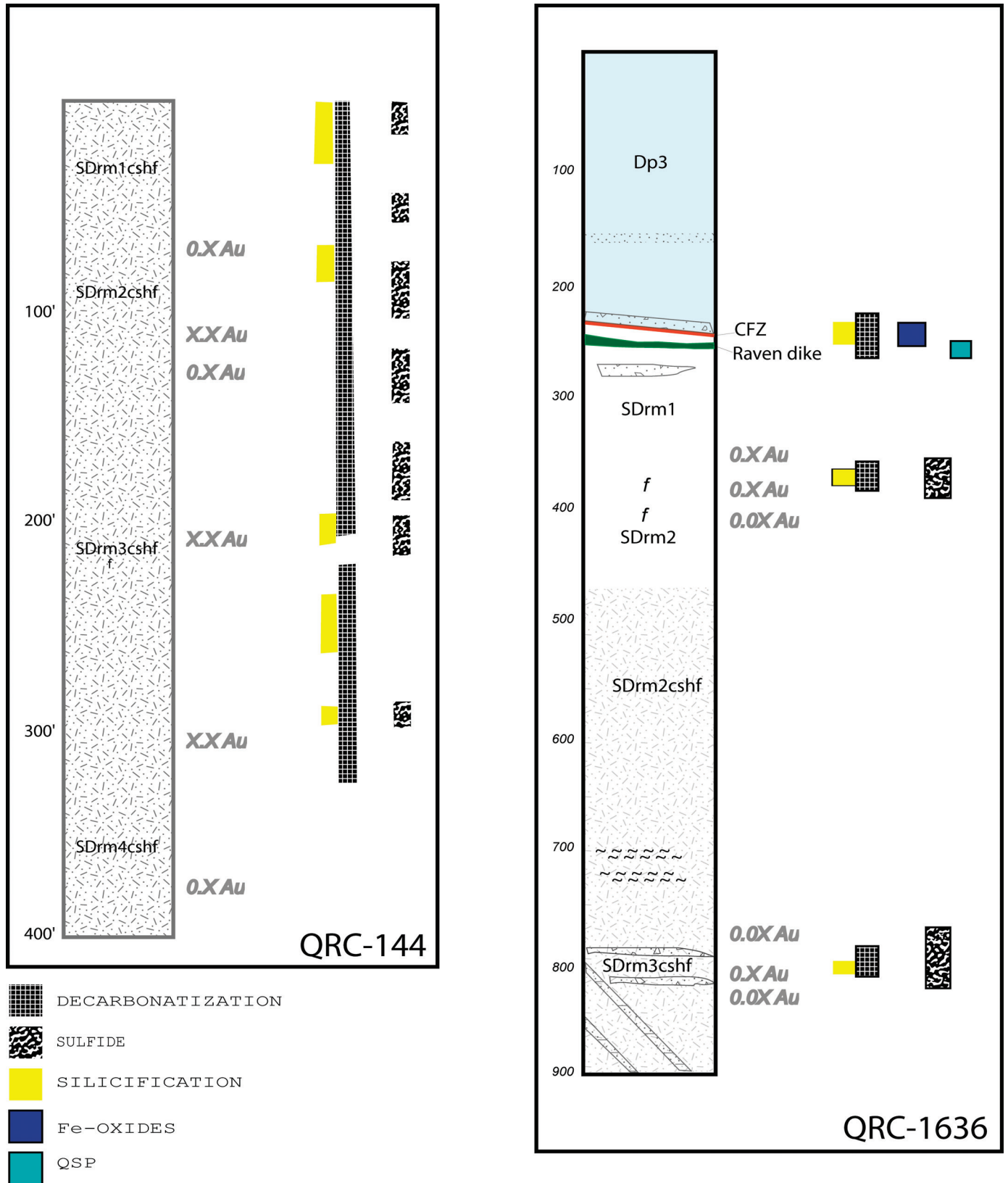


Figure 11. Core logs from drill-holes QRC-144( west limb) and QRC-1636 (east limb) showing ore grades and associated hydrothermal alteration. Note high grade mineralization hosted in calc-silicate hornfels in hole QRC-144 , a good example that carbonate rocks are not the exclusive host-rocks for hosting Carlin-type orebodies. Au values in opt (Core log data from Newmont, 2004).

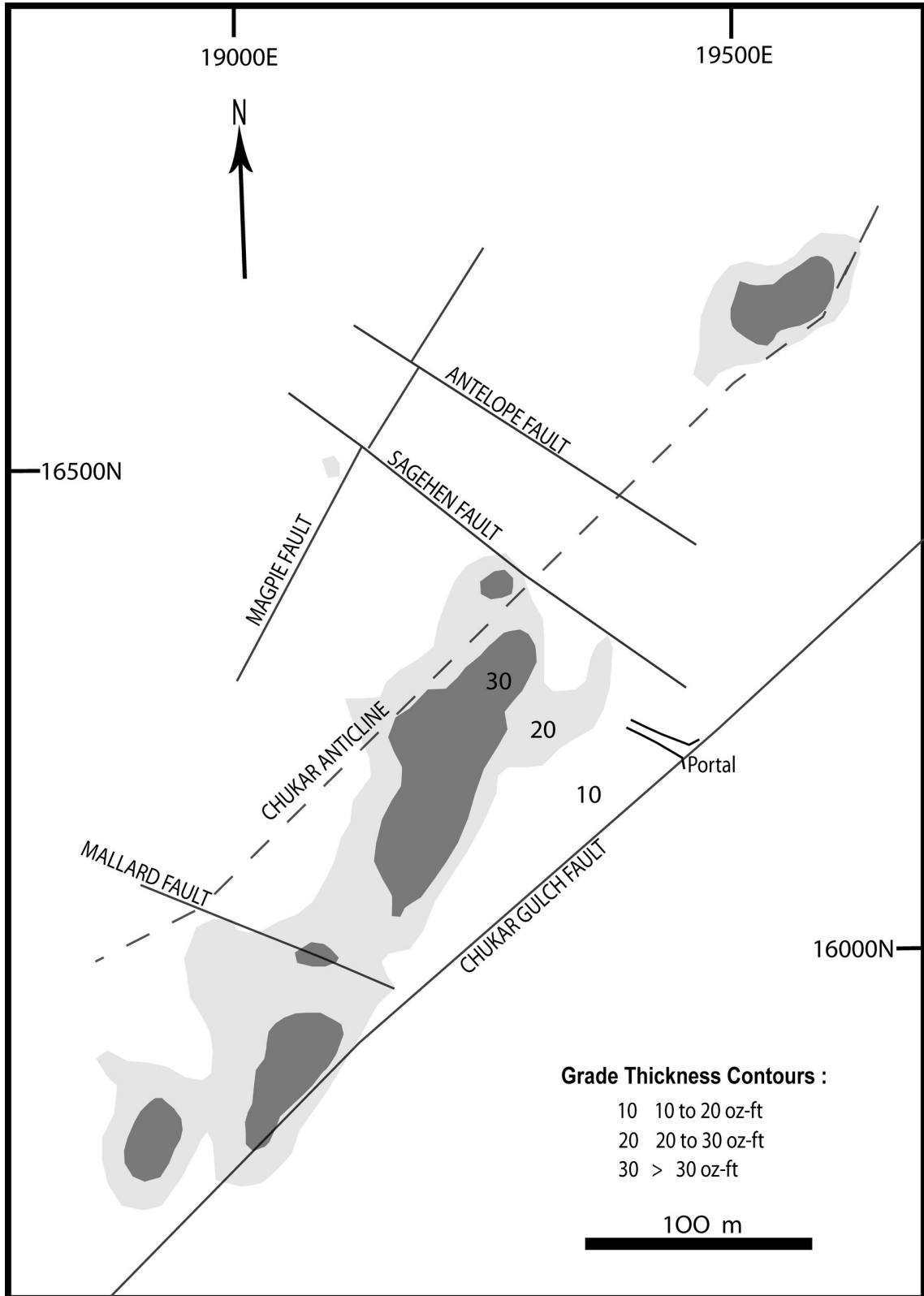


Figure 12. Grade thickness map of the Chukar Footwall mine. Approximate trace of the structures at the 4650 ft. elevation. Gold orebodies form two main sub-parallel linear trends: (1) the Chukar anticline trend and (2) the Magpie trend. The spatial distribution of gold orebodies relative to NE-striking structures and the east limb of the anticline show a strong structural control on the Chukar Footwall deposit ( Contour map from Newmont, 2004).

structural control of the Chukar Footwall with other deposits in the Carlin trend suggests late Eocene to Oligocene wrench tectonics, which accommodated extension at both local and regional scales, produced large-scale fractures with dilatant zones that led to the channeling and ultimately the deposition of gold and other metals (Cole, 1995; Tosdal and Nutt, 1999).

High grade gold mineralization at Chukar Footwall mine correlates well with strong decarbonatization and relatively high sulfide content (up to 3 vol. percent sulfides; Joe Sagar, personal communication, 2004). Silicification and dolomitization do not appear to be controls on gold grades. Another metallogenic characteristic of Chukar Footwall is that gold mineralization is hosted in both limestone and calc-silicate hornfels, reinforcing the concept pointed out by Thompson (2000) that carbonate lithologies are not the exclusive hosts for gold mineralization on the Carlin trend. Geochemically, the economic gold orebody at Chukar Footwall exhibits anomalous concentrations, relative to unmineralized fresh rocks, of As, Fe, and Sb (Fig. 10), with As and Fe as excellent pathfinders. Finally, although a genetic model for Chukar Footwall is still pending, field data point toward selective sulfidation processes and high diagenetic iron sulfides concentrations as being responsible for the deposition of the micron gold. A possible depositional mechanism(s) for the coarse, visible gold at the upper mine levels would be related to oxidation of auriferous bisulfide solutions leading to sulfate and Au precipitation.

## CONCLUSIONS

Although this research is still in progress, some general conclusions can be drawn based on the above body of data:

1. The host rocks at Chukar Footwall mine are the Roberts Mountains Formation, the Popovich Formation, and the Raven dike. Economic gold orebodies are hosted in the SDRm units.
2. The structural paragenesis is characterized by early, high angle ENE-striking oblique normal faults, followed by NE-striking faults. Cutting both systems are the NW- and NNW-striking structures. Both the Chukar Gulch fault and the CFZ are the structural limits of the deposit.
3. As, Fe, and Sb show good correlation with gold. Fe and As seem to be good pathfinders.
4. The orebodies are somewhat aligned sub-parallel to the axial trace of the Chukar anticline. The spatial distribution of these orebodies shows a strong structural control, wherein high angle, NNE-striking structures (e.g., the Maggie fault) are the principal feeders that funneled ore fluids toward the Chukar anticline.
5. Decarbonatization and silicification are the main alteration types at Chukar Footwall, although volumetrically small dolomitization is also present. In general, high grades correlate well with (1) strong decarbonatization and (2) structural intersections of NNE-striking structures with the Chukar anticline limbs.

## ACKNOWLEDGEMENTS

I would like to thank Dr. Tommy Thompson and Dr. Rich Schweickert for being my thesis advisors, and for their insights on the geological aspects of the Carlin trend.

Thanks to the Chukar Footwall geologists Joe Sagar and Kevin Creel for their logistical support, patience, and ideas about Chukar Footwall's geology during underground mapping. My appreciation is extended to Newmont for letting me work at Chukar Footwall, giving me free access to information, and conducting the ICP-MS analyses.

Finally, I would like to thank my fellow students Keith Campbell, Craig Mach, and Robert Wood for their help and ideas.

## REFERENCES

- Altamirano-Morales, C., 1999, Structural control and alteration at the Deep Star deposit, Eureka County, Nevada, [M.S. Thesis]: University of Nevada, Reno, 78 p., 1 plate.
- Arehart, G., Chryssoulis, S., and Kesler, S. 1993, Gold and arsenic in iron sulfides from sediment-hosted disseminated gold deposits: implications for depositional processes: *Economic Geology*, v. 88, p. 171–185.
- Arehart, G., 1996, Characteristics and origin of sediment-hosted disseminated gold deposits; a review: *Ore Geology Reviews*, v. 11, p. 383–403.
- Armstrong, A.K., Theodore, T.G., Oscarson, R.L., Kotlyar, B.B., Harris, A.G., Bettles, K.H., Lauha, E.A., Hipsley, R.A., Griffin, G.L., Abbot, E.A., and Cluer, J.K., 1998, Preliminary facies analysis of the Silurian and Devonian autochthonous rocks that host gold along the Carlin Trend, Nevada: U.S. Geological Survey Open-File Report 98-338, p.38–68
- Armstrong, A.K., Bagby, W.C., Ekburg, C., and Repetski, J., 1987, Petrographic and scanning electron microscope studies of samples from the Roberts Mountains and Popovich formations, Carlin Mine area, Eureka County, Nevada: U.S. Geological Survey Bulletin 1684, 23 p.
- Chakurian, A.M., 2001, Age of mineralization at the Carlin East Mine, Eureka County, Nevada [M.S. Thesis]: University of Nevada, Reno, 186 p.
- Craig, R.R., and Wakefield, T.W., 1991, Geochemistry of the Carlin Trend, in Craig, R., ed., *Geology and Geochemistry of the Carlin Trend: Association of Exploration Geochemists, Field Trip 4*, p. 1–7.
- Cress, L.D., 1972, Geology of the Carlin window area, Eureka County, Nevada [M.S. Thesis]: California State University, San Jose, 103 p.
- Cole, D.M., 1995, Structural evolution of the Gold Quarry deposit and implication for development, Eureka County, Nevada, [M.S. Thesis]: Colorado State University, Fort Collins, 78 p.
- Cook, H.E., and Corboy, J.J., 2002, Great Basin Paleozoic carbonate platform: facies, facies transitions, depositional models, platform architecture, sequence stratigraphy, and predictive mineral host models: U.S. Geological Survey Open-File Report 2004-1078, 129 p.
- Emsbo, P., Hofstra, A., Zimmerman, J.M., and Snee, L., 1996, A Mid-Tertiary age constraint on alteration and mineralization in igneous dikes on the Gold Strike property, Carlin Trend, Nevada: *GSA Abstracts with Programs*, v. 28, n. 7, p. A476.
- Ettner, D.C., 1989, Stratigraphy and structure of the Devonian autochthonous rocks, North-Central Carlin Trend of the Southern Tuscarora Mountains, Northern Eureka County, Nevada, [M.S. Thesis]: Idaho State University, Pocatello, 177 p.
- Evans, J.G., 1980, Geology of the Rodeo Creek and Welches Canyon quadrangles, Eureka County, Nevada : U.S. Geological Survey Bulletin 1473, 81 p.
- Harlan, J.B., Harris, D.A., Mallette, P.M., Norby, J.W., Rota, J.C., and Sagar, J.J., 2002, Geology and Mineralization of the Maggie Creek District, in

- Thompson, T.B., Teal, L., and Meeuwig, R.O., eds, Gold deposits of the Carlin Trend: Nevada Bureau of Mines and Geology, Bulletin 111, p.115–142.
- Harris, M. and Radtke, A., 1976, Statistical study of selected trace elements with reference to geology and genesis of the Carlin gold deposit, Nevada: U.S. Geological Survey Professional Paper 960, 21 p.
- Heitt, D., Dunbar, W., Thompson, T., and Jackson, R., 2003, Geology and geochemistry of the Deep Star gold deposit, Carlin Trend, Nevada: *Economic Geology*, vo. 98, no. 6, p. 1107–1135.
- Henry, C.D. and Ressel, M.W., 2000, Eocene magmatism of northeastern Nevada: the smoking gun for Carlin-type gold deposits, in Cluer, J.K., Price, J.G., Struchsacker, E.M., Hardyman, R.F., and Morris, C., eds., *Geology and Ore deposits 2000: The Great Basin and Beyond*, Proceedings, p.365–388.
- Hofstra, A.H., and Cline, J.S., 2000, Characteristics and models for Carlin-Type gold deposits, in Thompson, T.B., ed., *Reviews in Economic Geology: Society Economic Geologists*, v. 13, p. 163–220.
- Hutcherson, S., 2002, *Geology, Geochemistry and Alteration of Zone 5 of the Murray Mine, Jerritt Canyon District, Elko County, Nevada*, [M.S. Thesis]: University of Nevada, Reno, 114 p., 4 plates.
- Ilchik, R.P., and Barton, M.D., 1997, An amagmatic origin of Carlin-Type gold deposits: *Economic Geology*, v. 92, p. 269–288.
- Jackson, M., Lane, M., and Leach, B., 2002, Geology of the West Leeville deposit, in Thompson, T.B., Teal, L., and Meeuwig, R.O., eds, *Gold deposits of the Carlin Trend: Nevada Bureau of Mines and Geology, Bulletin 111*, p.106–114
- Johnston, M.K. and Ressel, M.W., 2004, Carlin-Type and distal disseminated Au-Ag deposits: Related distal expressions of Eocene intrusive centers in north-central Nevada: *SEG Newsletter*, no. 59, p.12–14.
- Lewis, P., 2001, Structural analysis of gold deposits of the Carlin Trend, Elko and Eureka Counties, Nevada. Newmont Mining Corp. and Barrick Goldstrike Mines Inc. Internal Report, 166 p.
- McComb, M., 1993, Petrographic examination and semiquantitative XRD-XRF analysis of Gold Quarry dike rocks: Newmont Exploration Ltd., Memorandum to D. Pietz, November 23, 1993, 19 p.
- Mariño, F.A., 2003, *Geology of the Deep Post mine, Northern Carlin Trend, Nevada*, [M.S. Thesis]: University of Nevada, Reno, 118 p.
- Mullens, T.E., 1980, Stratigraphy, Petrology, and Some Fossil Data of the Roberts Mountains Formation, North-Central Nevada: U.S. Geological Survey Professional Paper 1063, 67 p.
- McCrossan, R.G., 1958, Sedimentary “boudinage” structures in the Upper Devonian Ireton Formation of Alberta: *Journal of Sedimentary Petrology*, v. 28, p. 316–320.
- Moore, S., 2001, Ages of fault movement and stepwise development of structural fabrics on the Carlin Trend: Regional tectonics and structural controls of ore: The major gold trends of Northern Nevada: *Geological Society of Nevada Special Publication 33*, p. 71–89.
- Newmont, 2003, Chukar Footwall, Geologic map at 4650 elevation, 1/1,200
- Newmont, 2004, Chukar Footwall. Grade Thickness Map, 1/1,200
- Norby, J.W. and Orobona, M.J., 2002, Geology and minerals systems of the Mike deposit, in Thompson, T.B., Teal, L., and Meeuwig, R.O., eds, *Gold deposits of the Carlin Trend: Nevada Bureau of Mines and Geology, Bulletin 111*, p.143–167.
- Radtke, A. S., 1985, *Geology of the Carlin gold deposit, Nevada: U.S. Geological Survey Professional Paper, 1267*, 124 p.
- Ramsay, J. and Huber, M., 1987, *The Techniques of Modern Structural Geology, Volume II: Folds and Fractures: Academic Press*, 700 p. Academic Press, London, 700 p.
- Ressel, M., Noble, D., Henry, C., Trudel, W., 2000, Dike-hosted ores of the Beast deposit and the importance of Eocene magmatism in gold mineralization of the Carlin trend, Nevada: *Economic Geology*, v. 95, no.7, p. 1417–1444.
- Roberts, R.J., Hotz, P.E., Gilluly, J., and Ferguson, H.G., 1958, Paleozoic rocks of North-Central Nevada: *American Ass. Petroleum Geologist Bulletin*, v. 42, no. 12, p. 2813–2857.
- Roberts, R.J., 1960, Alignment of mining districts in North-Central Nevada: *Geological Survey Professional Papers 400-B*, p. B17–B19.
- Sagar, J.J, 2000a, The Chukar Footwall model. Newmont Internal Report, 7p.
- Sagar, J.J., 2000b, Gold Quarry mine tour: *Geological Society of Nevada Symposium Geology and Ore deposits 2000*, p. 81–83.
- Seedorff, E., 1991, Magmatism, extension, and ore deposits of Eocene to Holocene age in the Great Basin—Mutual effects and preliminary genetic relationships: *Geology and ore deposits of the Great Basin Symposium, Geological Society of Nevada, Reno, Proceedings*, p. 133–178.
- Sha, P., 1993, *Geochemistry and genesis of sediment-hosted disseminated gold mineralization at the Gold Quarry mine, Nevada*, [Ph.D. Dissertation]: University of Alabama, Tuscaloosa, 229 p.
- Stenger, D., Kesler, S., Peltonen, D., and Tapper, C., 1998, Deposition of gold in Carlin-type deposits: The role of sulfidation and decarbonation at Twin Creeks, Nevada: *Economic Geology*, vo. 93, p. 201–215.
- Ressel, M.W., Noble, D.C., Henry, C.D., and Trudel, W.S., 2000, Dike-hosted ores of the Beast deposit and the importance of Eocene magmatism in gold mineralization of the Carlin Trend, Nevada: *Economic Geology*, v. 95, p. 1417–1444.
- Rota, J.C., 1991, A review of Gold Quarry geology, in Craig, R., ed., *Geology and Geochemistry of the Carlin Trend: Association of Exploration Geochemists, Field Trip 4*, p. 1–24.
- Teal, L. and Jackson, M., 2002, Geologic overview of the Carlin Trend gold deposits, in Thompson, T.B., Teal, L., and Meeuwig, R.O., eds, *Gold deposits of the Carlin Trend: Nevada Bureau of Mines and Geology, Bulletin 111*, p.9–19.
- Thompson, T.B., 2000, What are “Carlin-Type” gold deposits?: *GSA Abstracts with Programs*, v. 32, n. 7, p. A250.
- Tosdal, R.M. and Nutt, C.J., 1999, Late Eocene and Oligocene tectonic setting of Carlin-type Au deposits, Carlin trend, Nevada, USA, in Stanley and others, eds., *Mineral Deposits: Processes and Processing*, p.905–908.
- Tretbar, D., 2000, Controls on Gold Depositio in the 194 Orebody, a Collapse Breccia in the Getchell Mine, Humboldt County, Nevada: *Ralph J. Roberts CREG Annual Research Meeting, Program and Reports*, 49 p.
- Williams, C.L., 1992, Breccia bodies in the Carlin Trend, Elko and Eureka Counties, Nevada [M.S. Thesis]: Colorado State University, Fort Collins, 213 p.
- Williams, S.A, 2002, Petrographic report to Newmont, 4 p.
- Wilson, J.L., 1969, Microfacies and sedimentary structures in “deeper water” lime mudstones, in Friedman, G.M., ed, *Depositional environments in carbonate rocks: Society Economic Paleontologists and Mineralogists Special Publication 14*, p. 4–19.

## ADDENDUM

Geochronological data from the Raven dike (4580 level) produced an age of intrusion of  $200.3 \pm 5.1$  Ma from zircon U-Pb geochronology. Apatite fission-track dating yielded a date of  $20.6 \pm 4.5$  Ma from the same dike, suggesting the age for the thermal alteration responsible for the mineralization at Chukar Footwall mine.